Sixth International Symposium on Cavitation
CAV2006, Wageningen, The Netherlands, September 2006

INTERACTION OF A CAVITATION BUBBLE WITH A SPHERICAL FREE SURFACE

Farhat Mohamed[1], **Obreschkow** Danail[2], **Kobel** Philippe[3], **Dorsaz** Nicolas[1], **De Bosset** Aurel[1]
[1]Ecole Polytechnique Fédérale de Lausanne, 1015 Lausanne, Switzerland
[2]Physics Department, Oxford University, Oxford OX1 3PU, United Kingdom
[3]Max Planck Institute for Solar System Research, 37191 Katlenburg-Lindau, Germany

ABSTRACT

The dynamic of a cavitation bubble inside a water drop is investigated in microgravity in order to analyze the interaction between the collapsing bubble and a quasi-spherical free surface. Tests are carried in the frame of the 42nd parabolic flight campaign organized by the European Space Agency (ESA). High-speed visualization revealed a significant influence of isolated, finite liquid volumes and spherical free surfaces on the bubble growth and collapse In particular; collapsing bubbles eject two liquid jets escaping from the drop in antipodal directions. The bubble lifetime is significantly shortened in good accordance with a herein derived analog of the Rayleigh-Plesset equation for bubbles in water drops. The spherical free surface leads to a broader counter jet than previously studied for flat free surfaces. The shock waves generated at the bubble collapse are spatially confined, which leads to the formation of a large number of transient micro bubbles. This phenomenon is hardly visible in the ground based experiments when bubbles are collapsing near a flat free surface within a large liquid volume.

INTRODUCTION

The dynamic of a single cavitation bubble in still liquids has been widely investigated with variety of boundary conditions. It is well known that the nature of any neighboring wall highly influences the dynamic of the bubble during its growth and collapse through boundary conditions imposed on the surrounding pressure field. Both the erosion aggressiveness and the amount of light emission, which result from the cavity collapse, depend on the boundary conditions. When a cavitation bubble is set to grow and collapse in the vicinity of a rigid wall, hydrodynamic instabilities at the bubble interface lead to the generation of high speed micro jet, which threads the collapsing bubble as soon as the standoff parameter is below a critical value. Moreover, strong shock waves are also generated at the final stage of the bubble collapse as reported by many authors. Along with the micro-jet, these shock waves contribute in the erosion process. Tomita et. al. (2002) have investigated the effect of solid wall curvature on a collapsing bubble. They pointed out that when a vapor bubble collapses near a convex boundary, especially for high wall curvature, the jet velocity is significantly higher than that of the flat boundary case.

Unlike solid boundaries, the influence of a neighboring free surface has been less addressed in recent researches despite the tremendous work produced after the Second World War in the field of underwater explosions. It is well known that unlike solid walls, a collapsing bubble near a flat free surface moves away from the free surface and generates two jets in antipodal directions: the micro jet across the bubble and a counter jet out of the free surface. This is illustrated on Figure 1 where a spark generated bubble is visualized as it grows and collapse near a flat free surface at 6'000 frames/sec. The bubble collapses and rebounds several times as it moves away from the free surface. Blake et. al. (2003) developed a validated computation method for similar case study using boundary integral method. They have shown that the counter jet becomes narrower as the bubble approaches the free surface.

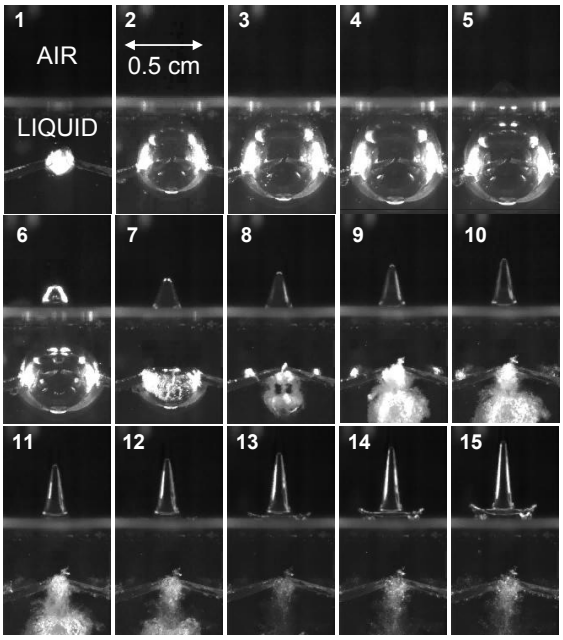

Fig. 1: Growth and collapse of a spark generated bubble near a flat free surface visualized at 6000 frames/s).

Besides the case of flat free surfaces, only few works addressed the influence of curved free surfaces on the cavity dynamic. Lettry et. al. (2003) and Robert (2004) have investigated the dynamic of eccentered bubble inside a liquid jet (cylindrical free surface) and pointed out the development of two opposite jets.

In the present study, the focus is put on a single bubble dynamics inside a quasi-spherical water drop produced in microgravity. The state of microgravity was achieved in parabolic flights (European Space Agency ESA). High-speed imaging allowed analyzing the implications of isolated and finite volumes and spherical free surfaces on bubble evolution, liquid jets formation and shock wave dynamics.

ZERO-G FLIGHT MANEUVER

The microgravity maneuvers were flown with the Airbus A300 zero-g, a specially equipped aircraft owned by NOVESPACE and hosted at the military airport Merignac in France. The standard flight maneuver is summarized in Figure 2. From a steady horizontal flight, the aircraft gradually pulls up its nose and climbs to an angle of approximately 45°. This pull up phase lasts for about 20 seconds, during which the aircraft experiences an acceleration of around 1.8 g, oriented perpendicularly to the wing plane. The engine thrust is then suddenly reduced to the minimum required to compensate for air drag, and the aircraft follows a free-fall ballistic trajectory, i.e. a parabola, lasting for approximately 20 seconds, during which weightlessness is achieved. At the end of this period, the aircraft must pull out of the parabolic period of 1.8 g. Finally it returns to a steady horizontal flight. These maneuvers are flown repeatedly, 32 times per flight day, with a rest period of 3 minutes between two consecutive parabolas.

EXPERIMENTAL SETUP

The experiment was carried out on two flight days, collectively containing 64 zero-g parabolas. Each parabola was used to create one spherical water drop within 5 to 15 s and to generate one short-lived cavitation bubble inside the drop at the end of its growth. Three physical parameters were independently varied: (1) drop size [radius = 8 to 13 mm], (2) maximal bubble size [radius = 3 to 10 mm], (3) bubble position within the drop. The experimental setup mainly consisted in a vessel containing the studied drop, two cameras and a flash light (see Fig. 3). Water drop growth and cavitation bubble evolution were recorded using a standard video-camera (25 frames/s) and an ultra fast CCD-camera (120’000 frames/s, Photron Ultima APX), respectively. The latter only filmed a short interval (11 ms) covering the bubble dynamics. This short sequence was illuminated by a perpendicularly placed high intensity flashlight (Cordin Light Source Model 359). A custom-designed computer program triggered the different experimental processes, such as drop creation, bubble generation, image recording and flash light release. The experimental cycle was initiated automatically at the beginning of each flight parabola, as soon as a stable level of microgravity (<0.005 g) was achieved. The respective gravity data was provided by a 100 Hz accelerometer that continuously recorded the gravity level during the whole flight.

The water drop was generated inside a transparent and sealed cubic vessel made of Perspex. It was smoothly expelled through a specially coated injector tube (see Figure 4, left) by means of a programmable micro-pump. In microgravity, the water volume naturally formed a truncated sphere due to surface tension (Fig. 5). The drop remained attached to the injector tube, which permitted to fix the drop’s position along the entire parabola and damped out eventual oscillations.

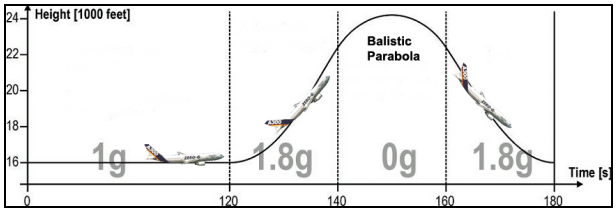

Fig. 2: The principle of parabolic flights

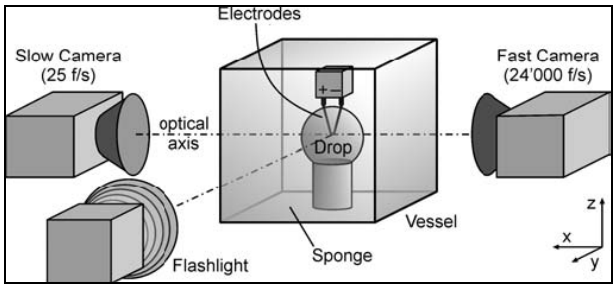

Fig. 3: The test section.

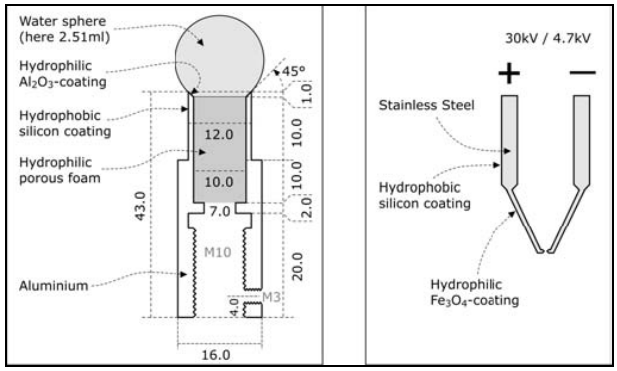

Fig. 4: Spherical water drop on injector tube in zero-g.

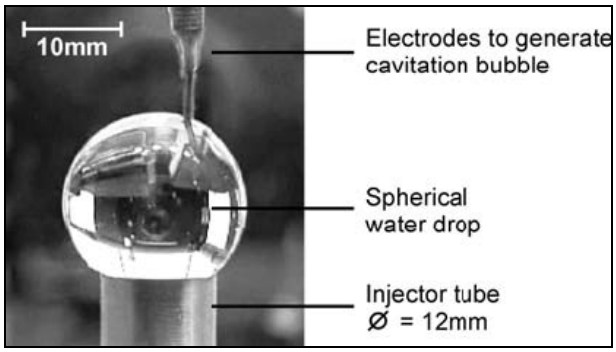

Fig. 5: Spherical water drop on injector tube in zero -g.

The cavitation bubbles were generated through electrical discharges between two electrodes immersed in the water drop (top of Fig. 3). Those electrodes where specially coated in order to minimize their interaction with the free-floating water drop (see Fig. 4, right). An initial high voltage between the electrodes (40 kV) formed plasma allowing the fast discharge of a previously charged capacitor with a capacitance of either 30 nF or 200 nF (charged at 4.7 kV). Shortly after this discharge, the plasma recombined, forming a volume of superheated water vapor that gave rise to a bubble (see Pereira et. al. 1994 for details on bubble generation). Using micro stages, the electrodes position could be precisely varied in the three space dimensions. Preliminary ground-based experiments were carried out to determine the fraction of the electrical discharge energy actually transformed in the cavitation bubble. Explicitly, single bubbles were generated inside water volumes that were much extended compared to the bubble

To characterize the bubble size and its location within the drop, we introduce the two dimensionless parameters. The relative radius of the bubble (α) and its eccentricity (ε):

$$\alpha = \frac{R_{b,\max}}{R_{d,min}} \qquad \varepsilon = \frac{d}{R_{d,min}}$$

where $R_{b,max}$ is the maximum radius of the bubble, $R_{d,min}$ is the initial radius of the drop and d is the distance between the bubble and drop centers.

RESULTS AND DISCUSSION

We have presented in Figure 6 the visualization of the growth and collapse of eccentrically placed bubble within a 20 mm diameter water drop. The relative radius of the bubble and its eccentricity are respectively 0.4 and 0.45. The frame rate is 12'000 frames/sec corresponding to 80 ms time step. The electric spark generated between the electrodes is well visible in the second frame of Figure 6. In the following frames the bubble grows and reaches its maximum radius after about 0.4 ms before starting its implosion. The first collapse occurs between frames N° 12 and 13 followed by a rebound of the cavity in a form of a cluster of micro bubbles. The cavity collapses and rebounds a second time between frames N° 20 and 21 and a third time between frames N° 27 and 28. The observation of the first collapse reveals that the nearby free surface breaks the spherical symmetry leading to a toroidal implosion with a fast micro jet directed perpendicularly away from the closest element of the drop interface. This micro jet accelerates the surrounding volume forming a jet that escapes from the right surface at a reduced velocity (6 m/s). In the meantime, a slower counter jet escapes in the opposite direction (Fig. 6, frame N° 40 to 90). This double-jet formation aligns with established studies of bubbles in the vicinity of free surfaces (see Robinson 2001 and Crum 1979), and provides the first direct visualization of both bubble-induced jets escaping from a steady liquid volume.

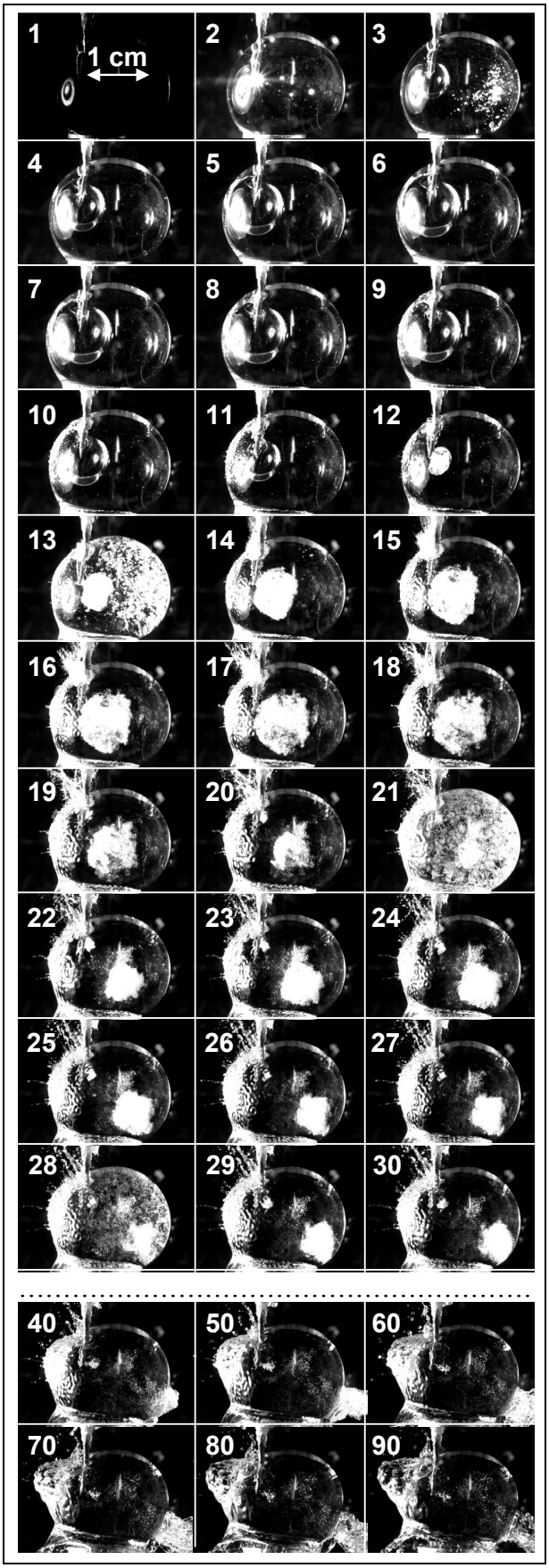

Fig. 6: Visualization of ignition, growth and collapse of a cavitation bubble inside a water drop. (time step=80 μs) α=0.3, ε=0.45

Close investigations of the counter jet geometry in the whole range ($0.2 < \alpha < 0.6$, $0.3 < \varepsilon < 0.8$) reproducibly revealed a remarkable diameter broadening compared to similar jets on ground-based experiments with flat free surfaces (see Fig. 1). For flat surfaces, the narrow counter jet results from a highly localized pressure peak between bubble and free surface (Pearson et. al. 2004). For a spherical free surface, the variation of the distance between bubble boundary and free surface is smoother. Hence, we believe that the high-pressure zone between bubble and free surface is stretched parallel to the surface leading to a broader counter jet. We also note that the typical crown surrounding the counter jet on flat surfaces (Fig. 1, frame N° 15) is absent on the spherical surface, a non-trivial feature, which presumably relates to viscous behavior.

The sequence presented in figure 6 also reveals a peculiar simultaneous appearance of a large number of short-lived brilliant micro bubbles on isolated frames. Such micro bubbles were systematically observed for all experimental conditions, and have typical diameters of 0.05 to 0.5 mm and lifetimes of 10 to 100 μs. They always precisely succeed the instants of predicted shock-wave radiation: The spark (or primary) shockwave is emitted before the bubble growth at the spark generation, and collapse (or secondary) shockwaves are radiated at the bubble collapse and subsequent collapses of rebound bubbles. The frames succeeding such collapses exhibit high density of micro bubbles within the drop. Although shockwaves were not directly visible with the present visualization setup, their exact synchronization with micro bubbles clearly discloses a shockwave related phenomenon. We believe that the micro bubbles originate from micro sized cavitation nuclei, which grow at the passage of shock-waves. The cavity-nature of micro bubbles was confirmed by showing that their size-lifetime ratio aligns with theoretical cavity life cycles. A surprising feature was the strong abundance of micro bubbles compared to faint traces seen in ground experiments. This difference is plausibly explained by the isolated drop volume, which can reflect a shock-wave many times with negligible energy loss across the free surface. Thereby the whole shockwave energy is transformed in micro bubbles by successive excitations. We may also observe in sequence of Figure 6 many tiny jets escaping from the drop interface after the first collapse. These jets originate from the micro bubbles that grow and collapse near the free surface after the passage of the main collapse induced shock wave. Indeed, the explanation given for the main cavity dynamic applies for these micro bubbles. Their collapse generate two jets: the micro jet and a counter jet directed outward the drop. Such a phenomenon is hardly observable in ground experiments since the confinement of shock waves is lacking.

In the following we consider the collapse of well centered bubbles ($\varepsilon = 0$), obtained with the electrodes positioned in the drop center. This configuration ensures spherical symmetry and allows for a consistent extension of the Rayleigh-Plesset model, governing bubbles in finite volumes. Bubbles with a relative radius $\alpha = 0.50$ were generated with discharge energies of 200 mJ and recorded at 50'000 frames/s with high optical definition (70 μm). A very good reproducibility was achieved with five samples all leading to the same collapse time of 330 μs +/- 10 μs. The evolution of the bubble radius $R_b(t)$, as reconstituted from the images using a correction model for optical refraction by a sphere, is plotted in Fig. 8 in dimensionless scales. The radius was normalized relative to its maximum value, whereas the time was normalized by the Rayleigh collapse time T_{Rayl} for bubbles in infinitely extended volumes (here at the cabin pressure of p_l = 80'000 Pa). A clear shortening of the collapse time for bubbles inside drops is revealed. For actual relative radius (α=0.5), the collapse time of the bubble is found to be less than 80% of the Rayleigh time.

In order to understand the shortening of the collapse time for cavities in drops, we have demonstrated (Obreschkow et. al., 2006) that the Rayleigh-Plesset model may be extended to address bubbles inside drops. With surface tension, liquid compressibility, viscosity and mass transfer across the bubble boundary being neglected, the mass and energy conservation in the liquid lead to the following differential equations, which correspond to the case of a bubble in infinite medium (1) and in the center of a water drop (2):

$$-\frac{\Delta p}{\rho} = \frac{3}{2}\dot{R}_b^2 + R_b \ddot{R}_b \qquad (1)$$

$$-\frac{\Delta p}{\rho} = \frac{3}{2}\dot{R}_b^2 + R_b \ddot{R}_b - 2\lambda \dot{R}_b^2 - \lambda R_b \ddot{R}_b + \frac{1}{2}\lambda^4 \dot{R}_b^2 \qquad (2)$$

with $\Delta p = p_\infty - p_V$, where p_∞ is the liquid pressure taken far from the bubble and ρ is the liquid density. The R_b is the bubble radius, λ is the ratio of bubble radius over the drop radius ($\lambda = R_b/R_d$).

Obviously, the gravity does not appear in both differential equations since it plays a minor role in the cavity dynamic. It should be noticed here that in our study, the microgravity is only intended to create the quasi spherical water drop to allow for the experimental investigations.

Equation (2) appears as an extension of the Rayleigh-Plesset equation (1) with three new corrective terms due to the water drop and which obviously vanish when the drop radius R_d becomes much larger than bubble radius ($\lambda \to \infty$). Integrating (2), provided the initial conditions $R_b(0)=R_{b;max}$ and $\dot{R}_b(0) = 0$, gives the radius evolution $R_b(t)$, which is independent of Δp and ρ in our normalized scales (Fig. 8, solid line). An excellent agreement of this curve with the microgravity data (circles) is obtained and proves that the shortened lifetime is entirely due to the finite spherical drop volume, and validates the derived equation of motion for bubbles centered in spherical drops (2).

We have applied the validated model to predict the collapse time $T_{collapse}$ of any bubble with arbitrary relative

radius α and shown that the integration of equation (2) provides the following expression (see Obreschkow et. al., 2006 for more details):

$$T_{collapse} = \xi(\alpha) R_{b,\max} \sqrt{\frac{\rho}{\Delta p}} \qquad (3)$$

with:

$$\xi(\alpha) = \sqrt{\frac{3}{2}} \int_0^1 \sqrt{1 - \frac{s}{\left(\alpha^{-3} + s^3\right)^{1/3}}} \left(\frac{1}{s^3} - 1\right)^{-\frac{1}{2}} ds$$

where s substitutes $R_b/R_{b;max}$. It appears that the collapse time depends on α through a collapse factor ξ(α) plotted in Figure 9. For infinite liquids (α = 0) we consistently recover the Rayleigh collapse factor ξ (0) = 0.915. ξ(α) decreases monotonously with increasing relative bubble radii α, tending to 0 for ($\alpha \to \infty$). This limit is non-physical since it violates the model assumptions. We have noticed that beyond a critical value of α ~ 0.53, the drop becomes unstable and starts to burst leading to a non spherical motion of the bubble interface.

CONCLUSION

The dynamic of a cavitation bubble inside a water drop is investigated in microgravity in order to analyze the interaction between the collapsing bubble and a quasi-spherical free surface. Tests are carried in the frame of the 42nd parabolic flight campaign organized by the European Space Agency (ESA). High-speed visualization revealed a significant influence of isolated, finite liquid volumes and spherical free surfaces on the bubble collapse and subsequent phenomena. The main conclusions may be summarized as follows:

- Collapsing bubbles eject two liquid jets escaping from the drop in antipodal directions.
- The spherical free surface leads to a broader counter-jet than previously studied flat free surfaces.
- The ratio between bubble radius and drop radius exhibits a stability limit, R_{bubble}/R_{drop}~0.53, beyond which the whole drop bursts.
- Bubble lifetime is significantly shortened in a good accordance with a herein derived analog of the Rayleigh-Plesset equation for bubbles in water drops.
- The confinement within the drop of bubble induced shock waves amplifies the formation of transient micro-bubbles. This phenomenon is hardly visible in ground based experiments with flat free surfaces.

ACKNOWLEDGMENTS

We gratefully acknowledge the European Space Agency (ESA) for having offered the possibility to pursue these experiments on parabolic flights. Our gratitude is also directed to the Swiss National Science Foundation (Grant No. 2000-068320), who provided the substantial basis of the whole research frame.

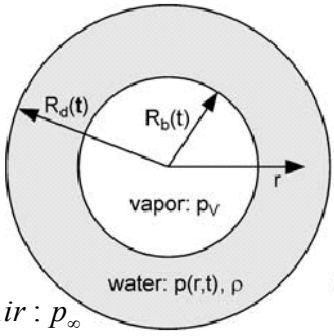

Figure 7: Nomenclature for mathematical modeling

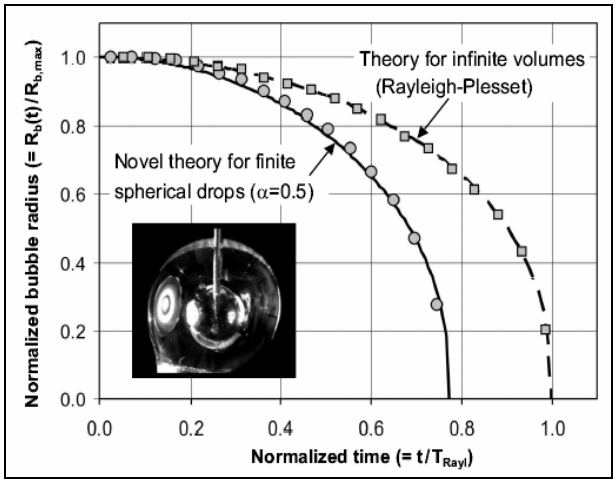

Fig. 8: Bubble radius during its collapse (α=0.5 and ε=0). Dashed line: Rayleigh theory. Squares: Ground-measurement in extended water volumes. Solid line: Modified theory for drops. Circles: Microgravity-measurements in water drops. Measurement errors are given by the height of the circles and squares.

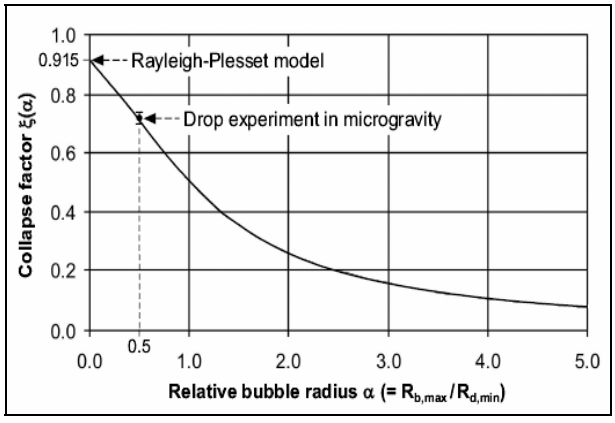

Fig. 9: Collapse factor ξ(α) as a function of the relative bubble radius α

REFERENCES

Obreschkow D., Kobel P., Dorsaz N., De Bosset A., Nicollier C., and Farhat M., " Cavitation Bubble Dynamics inside Liquid Drops in Microgravity", Physical Review Letters, to be published in September 2006.

Robert E, "Dynamic of a cavitation bubble inside a liquid jet", Master Thesis EPFL LMH. 2004.

A. Pearson, E. Cox, J. R. Blake and S. R. Otto, Engineering Anal. Bound. Elem. 28, 295 (2004)

Blake J. R., Pearson A. and Otto S. R., "Boundary Integral Methods for Cavitation Bubbles Near Boundaries", Cavitation 2003 symposium, Passadena, USA.

Lettry J, Fabich A, Gilardoni S, Benedikt M, Farhat M, Robert E. Journal of Physics G: Nuclear and Particle Physics 29(8): 1621-1627. 2003.

Wolfrum B, Kurz T, Mettin R, Lauterborn W. , "Shock wave induced interaction of microbubbles and boundaries", PHYSICS OF FLUIDS 15 (10): 2916-2922 OCT 2003

Tomita Y., Robinson P. B., Tong R. P. & Blake J. R., 'Growth and collapse of cavitation bubbles near a curved rigid boundary', J. Fluid Mech., vol. 466, pp. 259-283., 2002.

R. B. Robinson, J. R. Blake, T. Kodama, A. Shima, and Y. Tomita, "Interaction of cavitation bubbles with a free surface", J. Appl. Phys. 89, 8225 , 2001.

Kodama T, Tomita Y. Applied Physics B-Lasers and Optics 70 (1): 139-149, p. 147 (2000)

Shima A. Shock Waves 7: 33-42 , 1997

Brennen C E. Text book "Cavitation and Bubble Dynamics", chapter 5, Oxford University Press, 1995

Pereira F, Farhat M, Avellan F. "Dynamic calibration of transient sensors by spark generated cavity" in "Bubble Dynamics and Interface Phenomena", 227-240. J.R. Blake et al. (eds.). 1994.

Crum LA, Journal de Physique 41: 285-288 Suppl. 8, 1979.

Plesset, M.S. & Chapman, R.B., "Collapse of an initially spherical vapour cavity in the neighbourhood of a solid boundary", Journal of Fluid Mechanics, 1971, Vol. 47 , pp 283 – 290.